

Supporting information

Affecting surface chirality via multicomponent adsorption of chiral and achiral molecules

Zongxia Guo, Inge De Cat, Bernard Van Averbek, Jianbin Lin, Guojie Wang,
Hong Xu, Roberto Lazzaroni, David Beljonne, Albertus P. H. J. Schenning, Steven
De Feyter

1. Experimental Section

Synthesis. Details of the synthesis of OPV3Ts were reported before.¹ Thymine was bought from Carbosynth and used as received.

Scanning Tunneling Microscopy. All experiments were carried out at 20-25°C. Experiments were performed using a PicoSPM microscope (Agilent). Tips were mechanically cut from Pt-Ir wire (80:20 alloy, diameter 0.25 mm). Prior to imaging, the OPV3Ts and thymine were dissolved in 1-octanol (Anhydrous, 99+%, Sigma-Aldrich), and a drop of this solution was applied onto a freshly cleaved surface of highly oriented pyrolytic graphite (HOPG, grade ZYB, Advanced Ceramics Inc., Cleveland, OH). Almost all the STM imaging started at least 90 min after dropcasting to avoid interference of the initial dynamics at the liquid/solid interface. Images were recorded in the constant current mode. V_{set} refers to the sample bias. The graphite lattice was recorded by lowering the sample bias immediately after obtaining images of the monolayer. Drift effects were corrected via scanning probe image processor (SPIP) software (Image Metrology ApS).

Molecular Modeling. The physisorption of the adlayers on graphite was modeled by means of a Molecular Mechanics/Molecular Dynamics (MM/MD) approach. The DREIDING force field,² as implemented in the FORCITE tool pack of Materials Studio, was used, since it is particularly adapted to account for the hydrogen bonds that promote the self-assembly of the molecules. To validate the force field for the estimation of adsorption energies, we have considered a series of alkane molecules, for which experimental data are available in literature.³ The force field calculations were performed on model systems including OPV3Ts and thymine molecules in a 1:1 ratio deposited on graphite. The initial geometric configurations were inspired from assembly models based on the STM measurements. These were then subjected to energy minimization at 0K, releasing step by step all constraints imposed during the construction of the assemblies, followed by MD simulations in the NVT ensemble at 298K for 1ns. The long-range non-bonded interactions were turned off with a cubic spline cutoff set at 18 Å.

2. Self-assembly of the OPVs

Previous research revealed that these OPV-derivatives, both the chiral and achiral ones, can form well-defined monolayers composed of supramolecular cyclic hexamers (rosette structures) (Figure 1 and Figure S1) at the liquid/solid interface, as revealed by scanning tunneling microscopy (STM). Depending on the absolute configuration of the chiral centers in the OPV3T molecules, so-called clockwise (CW) and counterclockwise (CCW) rosettes are formed. This assignment refers to the relative orientation of the OPV units in the rosettes. Although A-OPV3T is an achiral molecule, it also can form chiral patterns and domains in a monolayer with conglomerates composed of CW and CCW rosettes.⁴ The rosettes formed by the chiral OPV-compounds, *S*-OPV3T and *R*-OPV3T, are related by mirror-symmetry (CW for *S*-OPV3T and CCW for *R*-OPV3T).⁵ For both achiral and chiral OPVs, a rosette consists of six OPV molecules (bright rod in the image), held together by hydrogen-bonds.

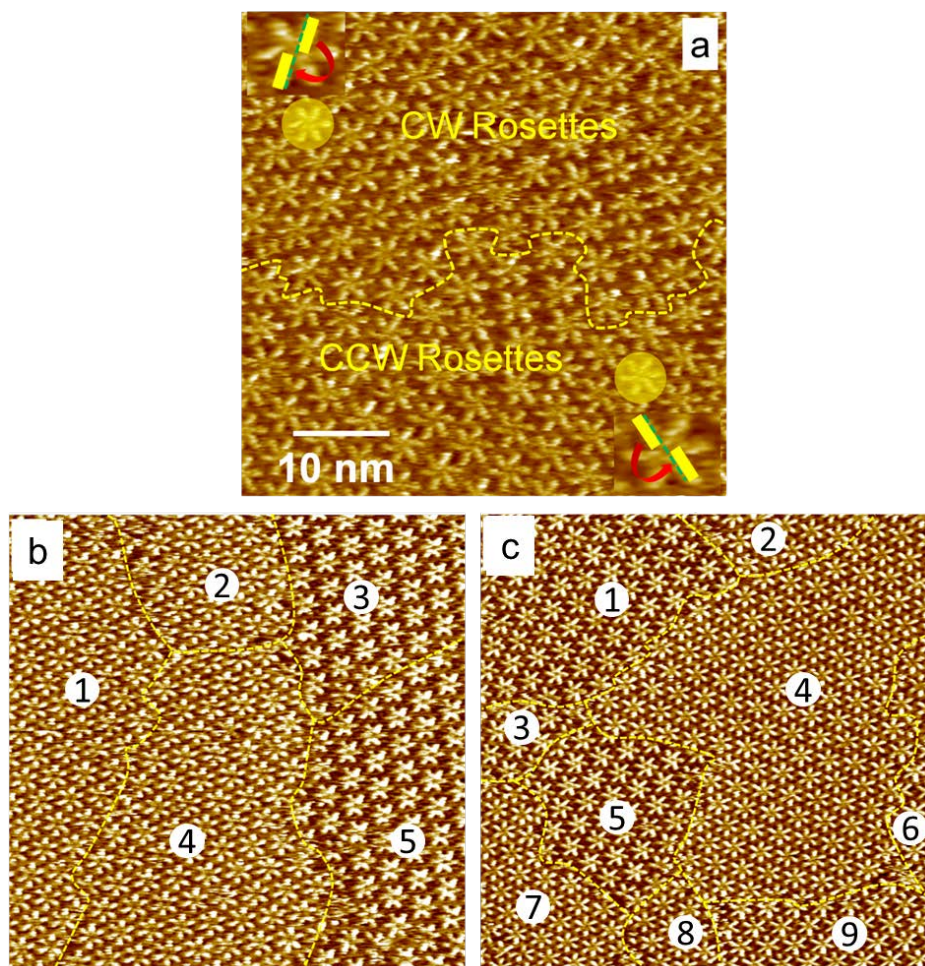


Figure S1. STM-images of A-OPV3T (a), *S*-OPV3T (b), and *R*-OPV3T (c) at the 1-octanol/HOPG interface. Size of the image is 80×80 nm². [OPV3T] = 1.0 mM.^{4, 5}

3. Thymidine-induced self-assembly of the achiral and chiral OPV derivatives

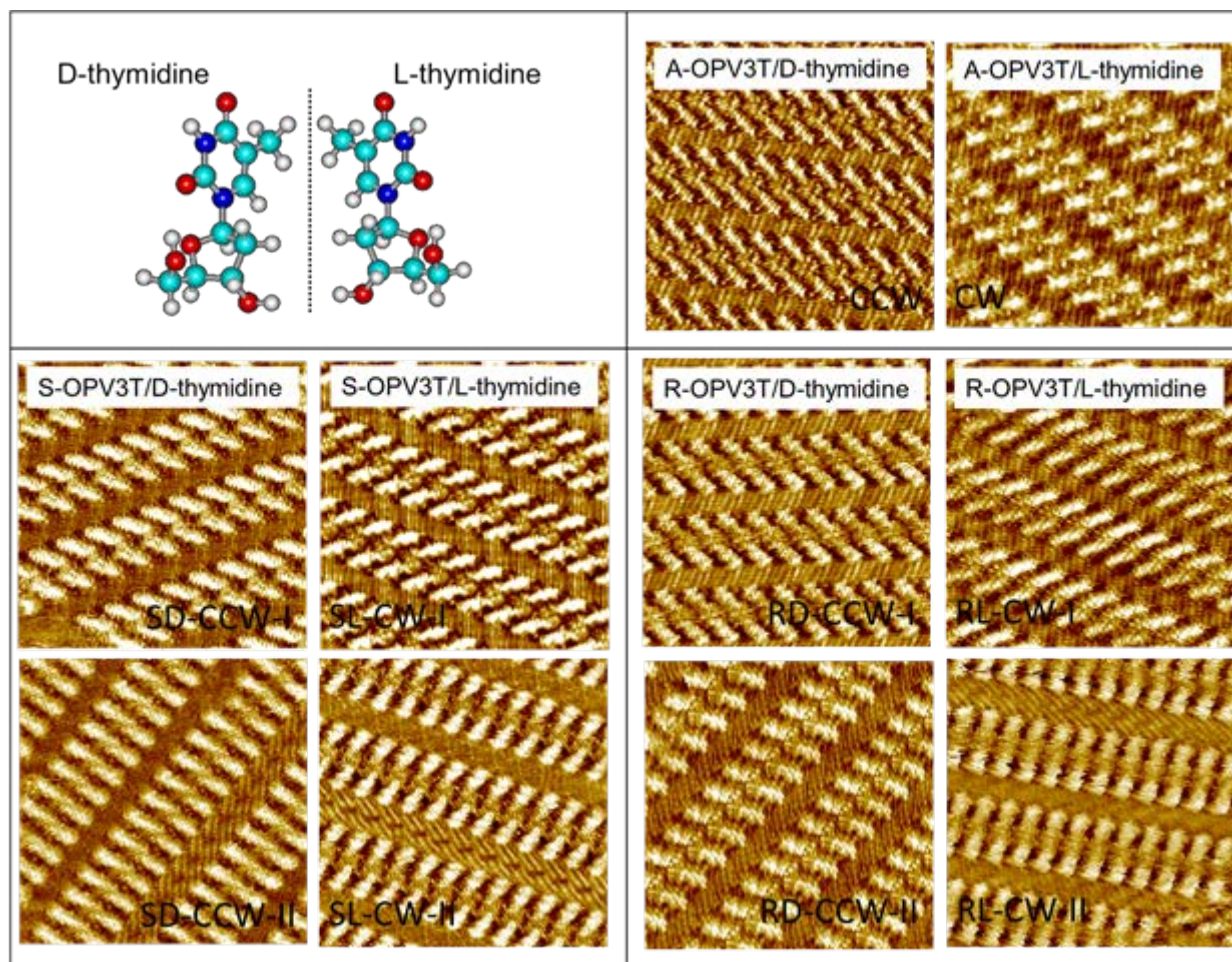


Figure S2. Structures of thymidine enantiomers and STM images of the 'dimers' formed from A-OPV3T/thymidine, S-OPV3T/thymidine, and R-OPV3T/thymidine mixtures at the 1-octanol/HOPG interface.^{4, 5}

4. Ratio-dependent self-assembly of achiral or chiral OPV and thymine

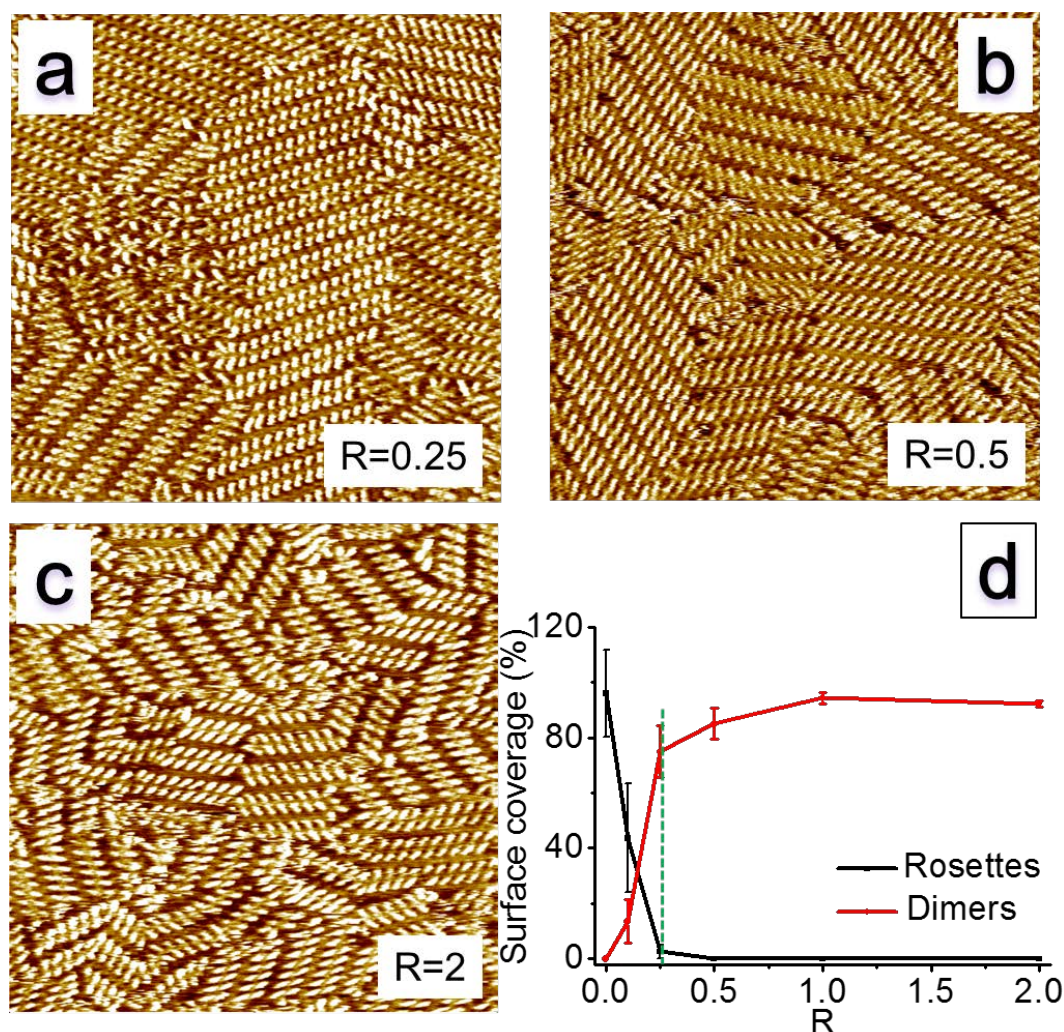


Figure S3. Molar ratio dependent pattern transformation of A-OPV3T at the 1-octanol/HOPG interface with the addition of thymine. $R = [\text{thymine}]:[\text{A-OPV3T}]$. $[\text{A-OPV3T}] = 1.0 \text{ mM}$. (a) $R = 0.25$, $I_{set} = 0.4 \text{ nA}$, $V_{set} = -0.28 \text{ V}$. (b) $R = 0.5$, $I_{set} = 0.6 \text{ nA}$, $V_{set} = -0.3 \text{ V}$. (c) $R = 2.0$, $I_{set} = 0.45 \text{ nA}$, $V_{set} = -0.26 \text{ V}$. (d) Surface coverage of rosettes and dimers as a function of R . STM image size is $60 \times 60 \text{ nm}^2$.

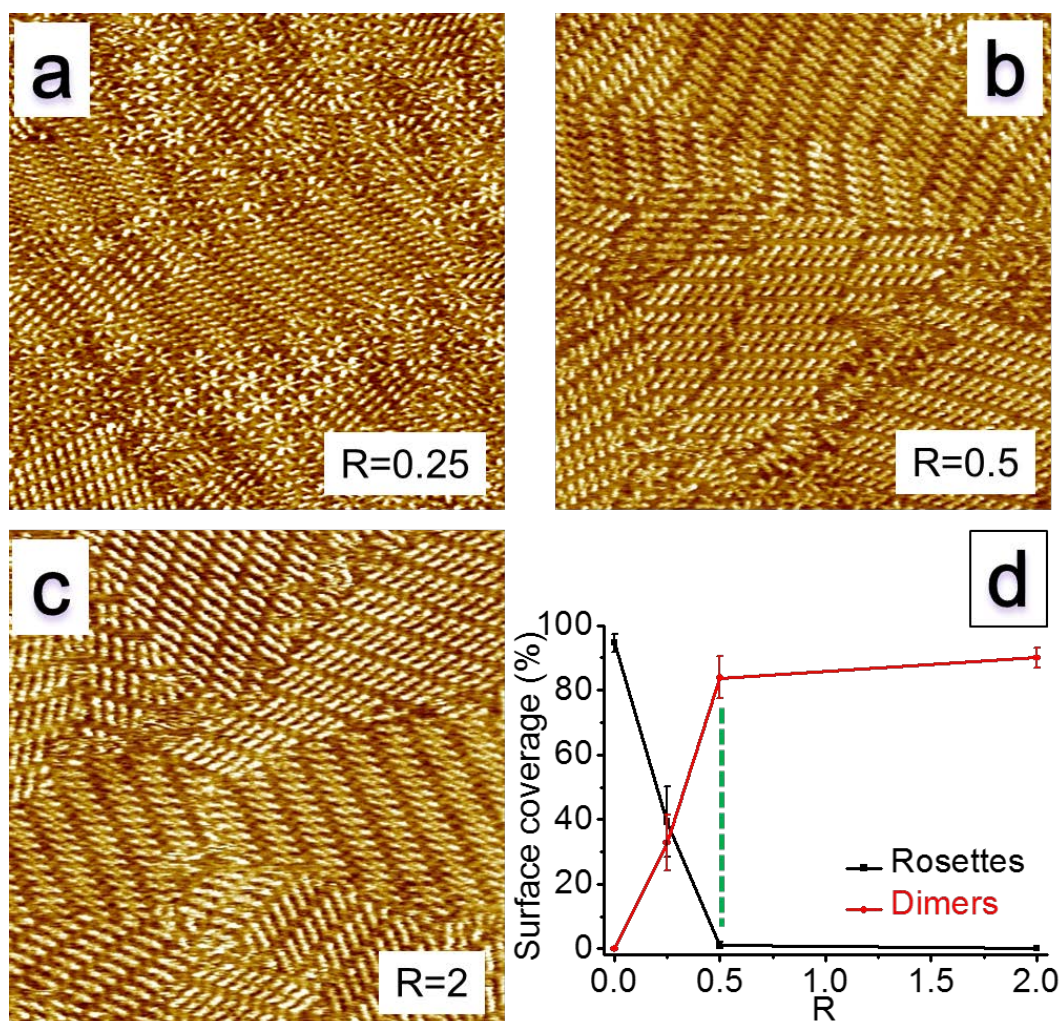


Figure S4. Molar ratio dependent pattern transformation of *S*-OPV3T at the 1-octanol/HOPG interface with the addition of thymine. $R = [\text{thymine}]:[S\text{-OPV3T}]$. $[S\text{-OPV3T}] = 1.0 \text{ mM}$. (a) $R = 0.25$, $I_{\text{set}} = 0.5 \text{ nA}$, $V_{\text{set}} = -0.28 \text{ V}$. (b) $R = 0.5$, $I_{\text{set}} = 0.14 \text{ nA}$, $V_{\text{set}} = -0.11 \text{ V}$. (c) $R = 2.0$, $I_{\text{set}} = 0.35 \text{ nA}$, $V_{\text{set}} = -0.19 \text{ V}$. (d) Surface coverage of rosettes and dimers as a function of R . STM image size is $60 \times 60 \text{ nm}^2$.

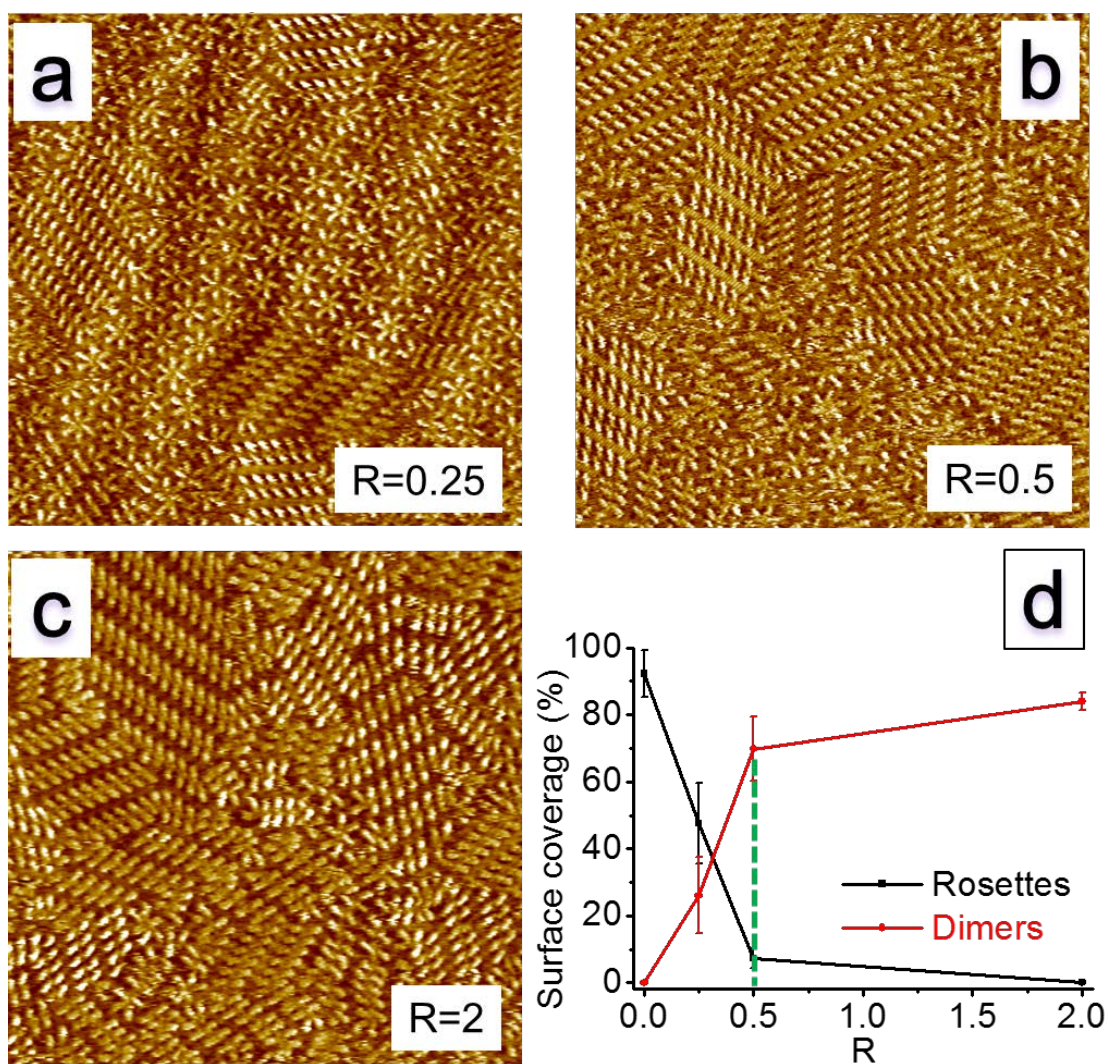


Figure S5. Molar ratio dependent pattern transformation of *R*-OPV3T at the 1-octanol/HOPG interface with the addition of thymine. $R = [\text{thymine}]:[\text{R-OPV3T}]$. $[\text{R-OPV3T}] = 1.0 \text{ mM}$. (a) $R = 0.25$, $I_{\text{set}} = 0.3 \text{ nA}$, $V_{\text{set}} = -0.27 \text{ V}$. (b) $R = 0.5$, $I_{\text{set}} = 0.45 \text{ nA}$, $V_{\text{set}} = -0.25 \text{ V}$. (c) $R = 2.0$, $I_{\text{set}} = 0.2 \text{ nA}$, $V_{\text{set}} = -0.23 \text{ V}$. (d) Surface coverage of rosettes and dimers as a function of R . STM image size is $60 \times 60 \text{ nm}^2$.

5. Defects in images

The monolayer patterns often contain defects. Figure S6 shows an image with defects which can't not be identified as dimers or rosettes.

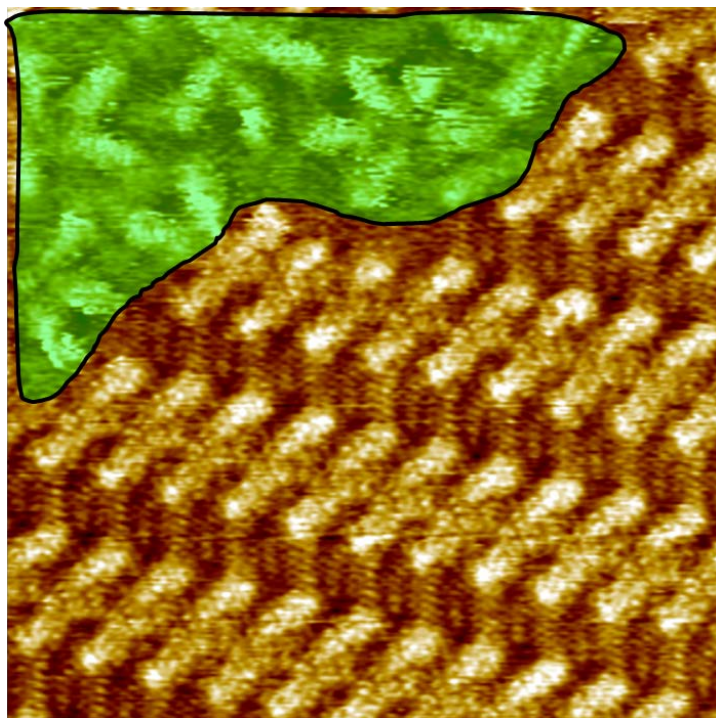


Figure S6. An STM-image of S-OPV3T with thymine at the 1-octanol/HOPG interface, $R = 0.25$ (thymine to OPV). $I_{set} = 0.9$ nA, $V_{set} = -0.001$ V. The defects are marked in green. Image size is 20×20 nm². [S-OPV3T] = 1.0 mM.

6. STM-image of AT when R=0.1 (thymine to OPV)

For the complex of A-OPV3T and thymine, even at very low molar ratio of thymine to OPV, there is considerable amount of dimer structures covering the HOPG surface. Figure S7 is a typical STM image at such condition.

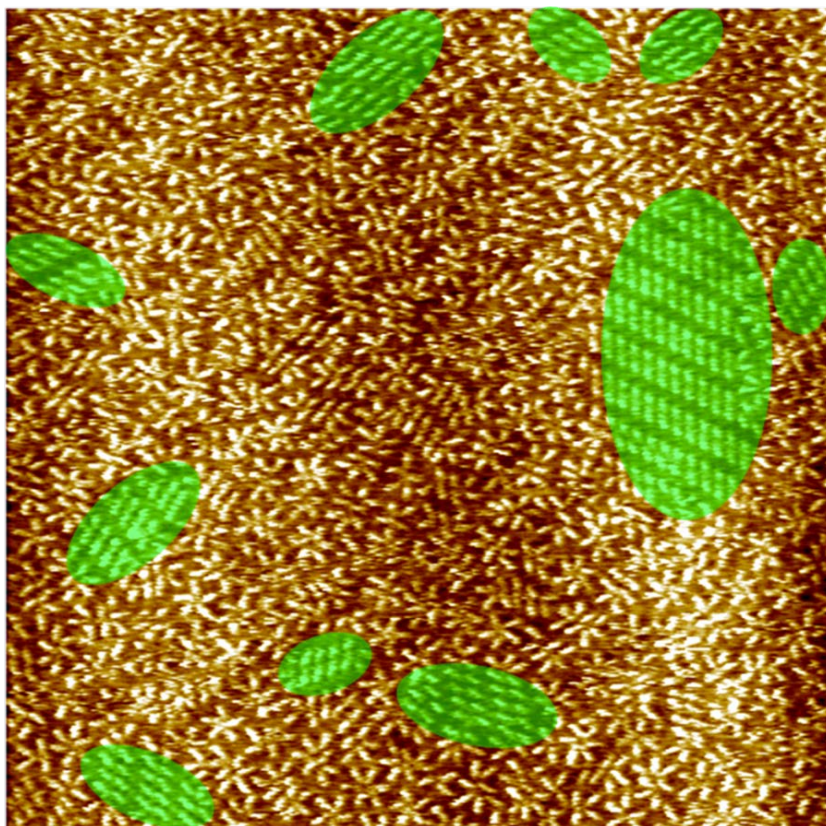


Figure S7. An STM-image of A-OPV3T with thymine at the 1-octanol/HOPG interface, $R=0.1$. $I_{set} = 0.35$ nA, $V_{set} = -0.27$ V. The dimers are marked by green color for clarity. Image size is 80×80 nm². [A-OPV3T] = 1.0 mM.

7. Molecular simulations

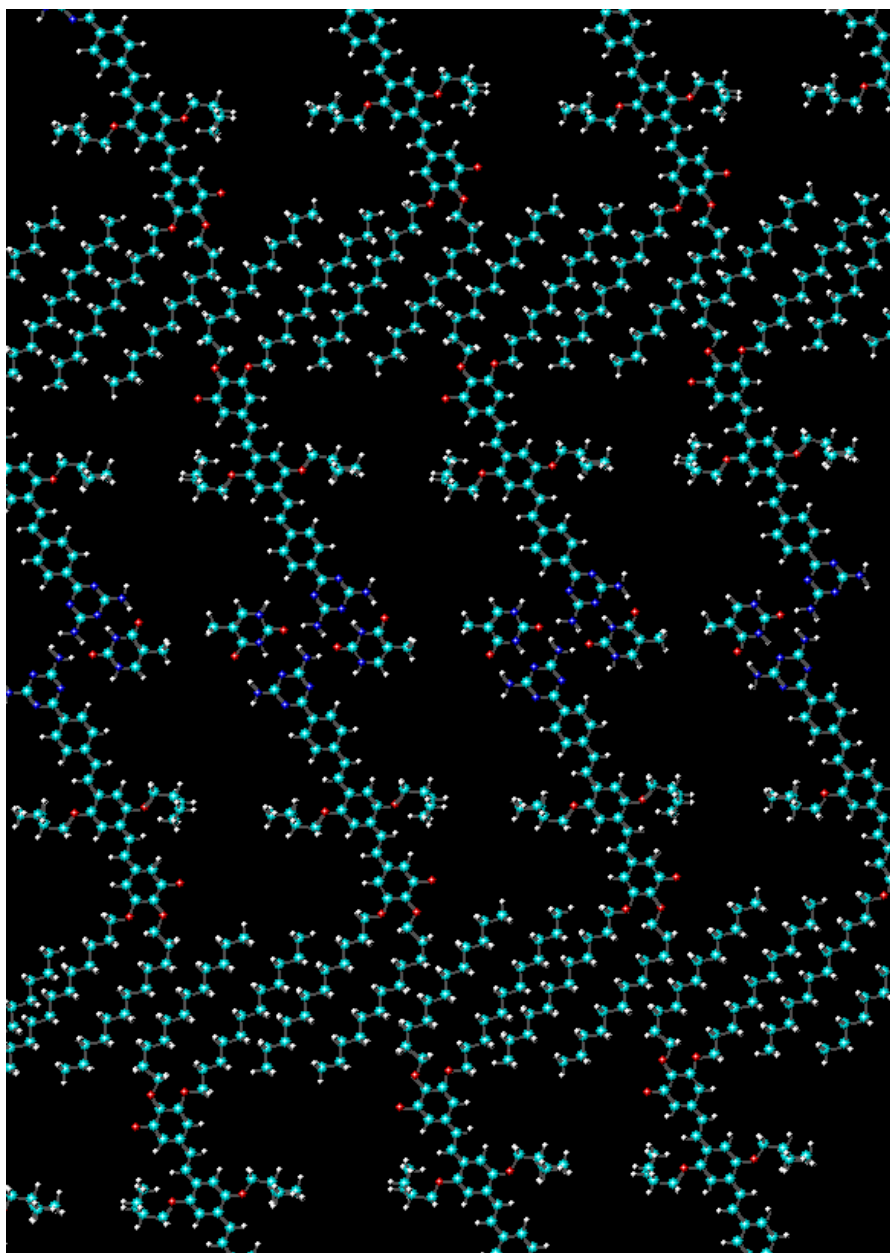


Figure S8. Simulated models for the monolayer of the CCW dimers for ST on graphite.

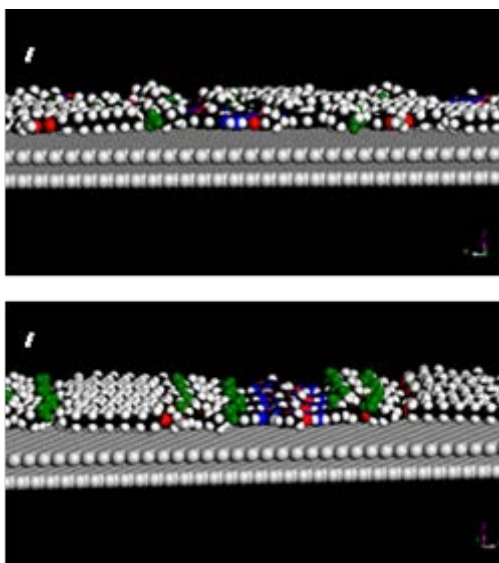


Figure S9. (a) CW dimers: methyl groups (in green) on the stereogenic center pointing down (to graphite). (b) CCW dimers: methyl groups on the stereogenic center pointing up.

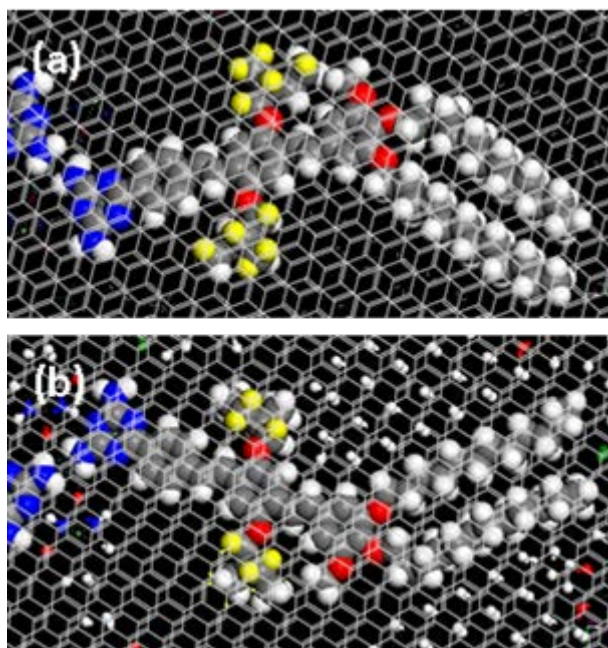


Figure S10. ‘Ball’ representation of one adsorbed OPV molecule, seen from beneath the graphite sheets (which are shown in a ‘stick’ representation). The neighboring molecules in the assembly are omitted for the sake of clarity. The hydrogen atoms of the stereogenic centers involved in CH- π interactions are shown in yellow. (a) CW dimers: 5 CH- π interactions per stereogenic center. (b) CCW dimers: 3 CH- π interactions per stereogenic center.

References

1. Wolffs, M.; George, S. J.; Tomovic, Z.; Meskers, S. C. J.; Schenning, A. P. H. J.; Meijer, E. W. *Angew. Chem., Int. Ed.* 2007, 46, 8203-8205.
2. Mayo, S. L.; Olafson, B. D.; Goddard, W. A. J. *Phys. Chem.* 1990, 94, 8897-8909.
3. Paserba, K. R.; Gellman, A. *J. Phys. Rev. Lett.* 2001, 86, 4338-4341.
4. Guo, Z.; De Cat, I.; Van Aeverbeke, B.; Lin, J.; Wang, G.; Xu, H.; Lazzaroni, R.; Beljonne, D.; Meijer, E. W.; Schenning, A. P. H. J.; De Feyter, S. *J. Am. Chem. Soc.* 2011, 133, 17764-17771.
5. (a) Minoia, A.; Guo, Z.; Xu, H.; Schenning, A. P. H. J.; George, S. J.; De Feyter, S. *Chem. Commun.* 2011, 47, 10924-10926. (b) Guo, Z.; De Cat, I.; Van Aeverbeke, B.; Ghijsens, E.; Lin, J.; Xu, H.; Wang, G.; Hoebe, F. J. M.; Tomović, Ž.; Lazzaroni, R.; Beljonne, D.; Meijer, E. W.; Schenning, A. P. H. J.; De Feyter, S. *J. Am. Chem. Soc.* 2013, 135, 9811-9819.